


First-Principles Investigation of Elastic, Electronic, and Half-Metallic Ferrimagnetic Properties in the Mn_2RhSi Heusler Alloy

Mostefa Zemouli¹ · Abdelkader Boudali¹ · Bendouma Doumi²  · Allel Mokaddem³ · Mohammed Elkeurti¹ · Fatiha Saadaoui¹ · Mohammed Driss Khodja¹

Received: 30 June 2016 / Accepted: 13 August 2016 / Published online: 24 August 2016
© Springer Science+Business Media New York 2016

Abstract The structural, elastic, electronic and magnetic properties of the Mn_2RhSi Mn_2 -based Heusler alloy were investigated by using first-principles calculations of the full-potential linearized augmented plane wave (FP-LAPW) method. The results of electronic structures show that the Mn_2RhSi exhibits a half-metallic character for a wide range 5.65 to 5.91 Å of lattice constant. The half-metallic behavior is confirmed by the integral value of $3 \mu_B$ of the total magnetic moment for Mn_2RhSi , which follow the Slater-Pauling rule.

Keywords Mn_2 -based Heusler alloy · Half-metallic ferrimagnetism · Slater-Pauling rule · Spintronics

1 Introduction

The Heusler alloys have attracted growing research interest because of their potential application as functional materials [1–3]. Numerous half-metallic Heusler alloys have been proposed using first-principles calculations, which are now known to exhibit a shape memory with interesting properties, where one of the most interesting of these materials

is the Mn_2 -based Heusler alloys. The half-metallic ferromagnetism has been discovered in several materials, like the ferromagnetic metallic oxides, dilute magnetic semiconductors, binary transition metal pnictides, chalcogenides with zinc blende structure, and Heusler compounds [4].

The Heusler alloys are important materials with respect to their interesting properties such as the electronic localization, itinerant magnetism, antiferromagnetism, helimagnetism, Pauli paramagnetism, or heavy-fermion behavior [5–8], and among these, the half-metallic property in Mn -based Heusler alloys is discovered in some theoretical and experimental studies. The half-metallic behavior was studied both theoretically [9–11] and experimentally [12] in Mn_2VAI . Besides, the half-metallicity is investigated in some Mn_2 -based Heusler alloys such as Mn_2VZ ($Z = \text{Si}, \text{Al}$) [13], Mn_2CoSn [14], Mn_2CoZ ($Z = \text{Al}, \text{Ga}, \text{In}, \text{Si}, \text{Ge}, \text{Sn}, \text{Sb}$) [15], Mn_2YAl ($Y = \text{V}, \text{Fe}, \text{Co}$) [16], Mn_2CoSb [17], and Mn_2FeZ ($Z = \text{Al}, \text{Ga}, \text{Si}, \text{Ge}, \text{Sb}$) [18] and in ferromagnetic shape memory alloys such as Mn_2NiGa [19] and Mn_2NiZ ($Z = \text{In}, \text{Sn}, \text{Sb}$) [20]. Although several studies have been devoted for the half-metallic ferrimagnets [21–29], the study of Wei et al. [25], for example, showed that the $\text{Mn}(1)$ and $\text{Mn}(2)$ atoms in the Mn_2CuGe alloy have large antiparallel spin moments with ferrimagnetic behavior. These materials are much more desirable than their ferromagnetic counterparts in magneto-electronic applications [30, 31]. Recently, the half-metallicity has been theoretically predicted for many of Mn_2 -based Heusler alloys [31–33].

To the best of our knowledge, there are no most works appeared on the electronic and magnetic properties of Mn_2RhSi Heusler alloy and there were no studies on the elastic properties of this compound. The purpose of this study is to predict the structural parameters, elastic constants, mechanical stability, electronic structure, and

✉ Bendouma Doumi
bdoummi@yahoo.fr

¹ Laboratory of Physico-Chemical Studies, University of Saida, Saida, Algeria

² Faculty of Sciences, Department of Physics, Dr. Tahar Moulay University of Saida, 20000 Saida, Algeria

³ Faculty of Physics, Department of Materials and Components, U.S.T.H.B., Algiers, Algeria

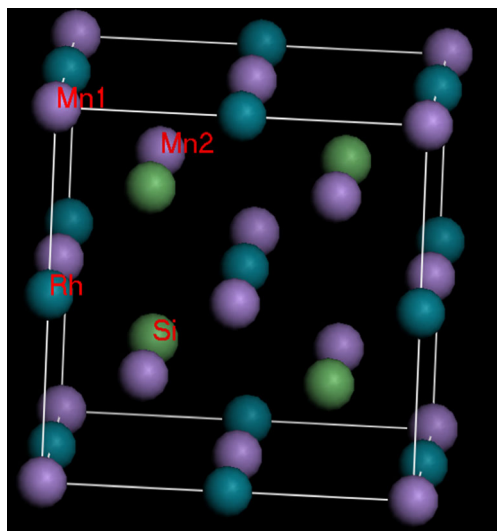


Fig. 1 The Mn_2RhSi Heusler alloy in the Hg_2CuTi -type structure with the atomic positions of Mn_1 (0, 0, 0), Mn_2 (1/4, 1/4, 1/4), Rh (1/2, 1/2, 1/2), and Si (3/4, 3/4, 3/4)

magnetic properties of Mn_2RhSi Heusler alloy. The calculations are carried out by using the first-principles calculations of the full-potential linearized augmented plane wave (FP-LAPW) method.

2 Method of Calculations

The electronic and magnetic properties are performed with the FP-LAPW method implemented in Wien2k code [34].

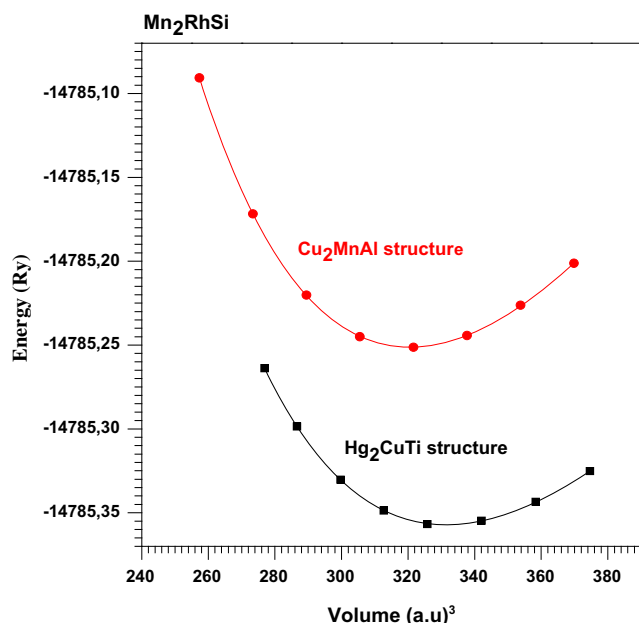


Fig. 2 Variation of total energy as a function of the volume (V) unit cell of Mn_2RhSi in the Cu_2MnAl - and Hg_2CuTi -type structures

Table 1 Calculated equilibrium energies of Mn_2RhSi in the optimized Cu_2MnAl and Hg_2CuTi structures

Compound	Energy (Ry) in the Cu_2MnAl -type structure	Energy (Ry) in the Hg_2CuTi -type structure
Mn_2RhSi	-14, 785.262	-14, 785.3446

The generalized gradient approximation (GGA) [35] is used for the exchange and correlation potential. The parameter $R_{\text{MT}} \times K_{\text{max}}$ (the smallest muffin-tin radius multiplied by the maximum k value in the expansion of plane waves in the basis set), which controls the size of the basis set in our calculations, is chosen to be equal to 8. The muffin-tin (MT) radii are chosen to be equal to 2.2, 2.3 and 2.06 a.u. for Mn, Rh, and Si, respectively. The basis set is expanded, within these spheres, with the charge density and potential in terms of the spherical harmonics up to the angular momentum $l_{\text{max}} = 10$. The Brillouin zone integrations for the total energy are carried out using 104 special k points in the irreducible Brillouin zone. The self-consistent convergence of the total energy was set at 0.1 mRy.

3 Results and Discussions

3.1 Structural Parameters, Elastic Properties, and Mechanical Stability

The X_2YZ Heusler alloys are ternary compounds, where X and Y are transition metals and Z is a group II, IV or V element [4]. The X_2YZ Heusler alloys crystallize into two possible structures: the Cu_2MnAl -type structure and the Hg_2CuTi -type structure. In the cubic Cu_2MnAl -type structure with the space group $Fm\bar{3}m$ (No. 225) the atoms are located at the Wyckoff coordinates: the X atoms occupy A (0, 0, 0) and B (1/2, 1/2, 1/2) sites, the Y atoms situated at the C site (1/4, 1/4, 1/4) and the Z atom situated at D site (3/4, 3/4, 3/4). In the Hg_2CuTi -type structure with the space group $F\bar{4}3m$ (No. 216), the X atoms occupy A (0, 0, 0) and B (1/4, 1/4, 1/4) positions while the Y and Z atoms are found in C (1/2, 1/2, 1/2) and D (3/4, 3/4, 3/4) positions, respectively [14] (see Fig. 1).

Table 2 Calculated structural parameters lattice constant (a), bulk modulus (B), and its pressure derivative (B'), for Mn_2RhSi

Compound	a (Å)	B (GPa)	B' (GPa)
Mn_2RhSi	5.761	211.81	4.87
Other calculations			
Mn_2RhSi	5.73 [33]		

Table 3 Calculated elastic constants C_{11} , C_{12} , and C_{44} ; the bulk modulus ($B = 1/3(C_{11} + 2C_{12})$); and the anisotropy factor (A) for Mn_2RhSi

Compound	C_{11} (GPa)	C_{12} (GPa)	C_{44} (GPa)	B (GPa)	A
Mn_2RhSi	288.54	179.99	155.57	216.17 (211.81)	2.866

The B values in parentheses are from the total energy optimization

The stability of the Mn_2RhSi compound in the Cu_2MnAl - or Hg_2CuTi -type structures must be known beforehand in order to calculate its structural properties. For Mn_2RhSi in the two Cu_2MnAl - and Hg_2CuTi -type structures, the lattice parameters are fully optimized at zero pressure as shown in Fig. 2. From Table 1, it can be seen that the equilibrium energy of the Cu_2MnAl -type structure is higher than that of the Hg_2CuTi -type, which indicates that Mn_2RhSi is energetically more stable in the Hg_2CuTi -type structure. This verifies the site preference rule of X and Y atoms, which is strongly affected by the number of their 3d electrons [16].

The calculated structural parameters of Mn_2RhSi in the Hg_2CuTi -type structure such as the lattice constant (a), bulk modulus (B), and its pressure derivative (B') with the available theoretical data [33] are listed in Table 2. The equilibrium lattice constant of Mn_2RhSi is 5.761, which is in agreement with the theoretical parameter found by Ren et al. [33].

The mechanical properties, such as the elastic constants (C_{11} , C_{12} , and C_{44}) and the Zener anisotropy factor (A) for Mn_2RhSi , were also calculated. The computed results are summarized in Table 3. Unfortunately, to our knowledge, no other results are available in the literature for comparison. In the present work, the elastic constants C_{11} , C_{12} , and C_{44} for the Mn_2RhSi were calculated by using the applied strains to be volume-conserving. To verify the structural stability of

our compound, we check the conditions for the mechanical stability criterion for cubic crystal [36–38]

$$C_{11} - C_{12} > 0, C_{11} > 0, C_{44} > 0, C_{11} + 2C_{12} > 0, \text{ and } C_{12} < B < C_{11} \tag{1}$$

Our results verify these conditions, indicating clearly that the Mn_2RhSi is stable in the Hg_2CuTi -type structure.

The Zener anisotropy factor (A) is an important parameter that measures the anisotropy of elastic wave velocity in a crystal structure; it is defined in the following expression [39]:

$$A = \frac{2C_{44}}{C_{11} - C_{12}} \tag{2}$$

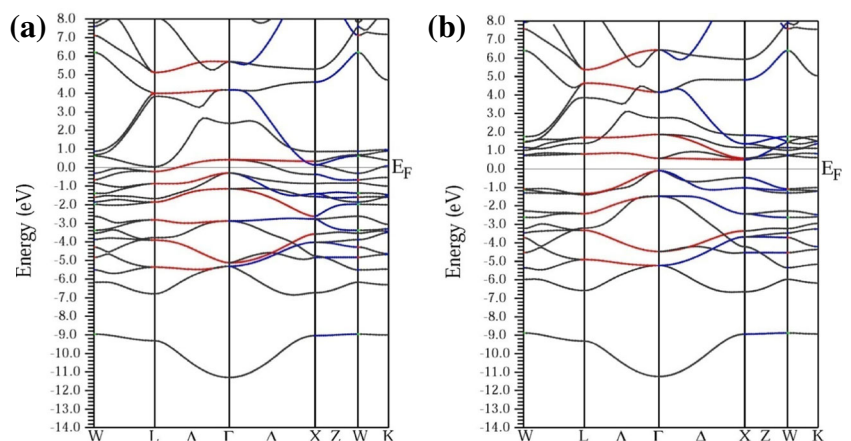
The anisotropy factors (A) for Mn_2RhSi verify the condition ($A > 1$), which implies that this compound is more rigid in the diagonal direction $<111>$ [40].

3.2 Electronic Properties

We have used the equilibrium lattice constant in the Hg_2CuTi -type to calculate the electronic and magnetic properties of Mn_2RhSi Heusler alloy. The spin-polarized band structures along high symmetry directions in the Brillouin zone for Mn_2RhSi are shown in Fig. 3. The minority-spin bands have an indirect bandgap along the Γ -X direction, showing a semiconducting character at the Fermi level, while the majority-spin bands depicted an intersection between valence and conduction bands at the Fermi level, indicating a metallic nature of the majority-spin channel. Thus, the Mn_2RhSi shows a half-metallic behavior.

To further elucidate the nature of the band structure of our material, their local density of state (LDOS) and total DOS (TDOS) were calculated. Figures 4 and 5 display respectively the trend of the total and partial densities of states for Mn_2RhSi . The TDOS depicts that majority-spin states are metallic, whereas the minority-spin states show the existence of a gap of 0.36 eV. Thus, the Mn_2RhSi behaves in

Fig. 3 Spin-polarized band structures for Mn_2RhSi at equilibrium lattice constant: **a** majority spin (*up*) and **b** minority spin (*down*)



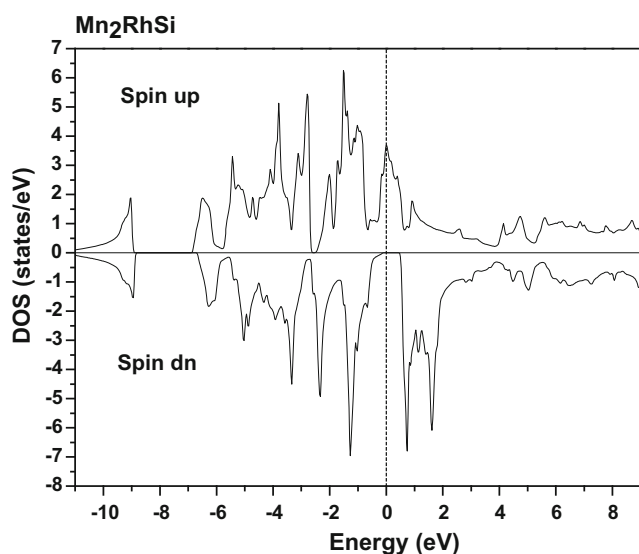


Fig. 4 Spin-polarized total density of states for Mn_2RhSi at equilibrium lattice constant

metallic nature for majority spin and a semiconductor for minority spin, inducing a perfect 100 % spin polarization at the Fermi level (E_F). This is due to the high value of the TDOS of spin-up at E_F . From Fig. 4 of TDOS, one can notice the existence of three peaks between -3 and 1 eV for the majority spin, which described the bonding and antibonding states of Mn atoms at E_F . For the minority spin, the gap stems from the large exchange splitting of the two Mn_1 and Mn_2 atoms.

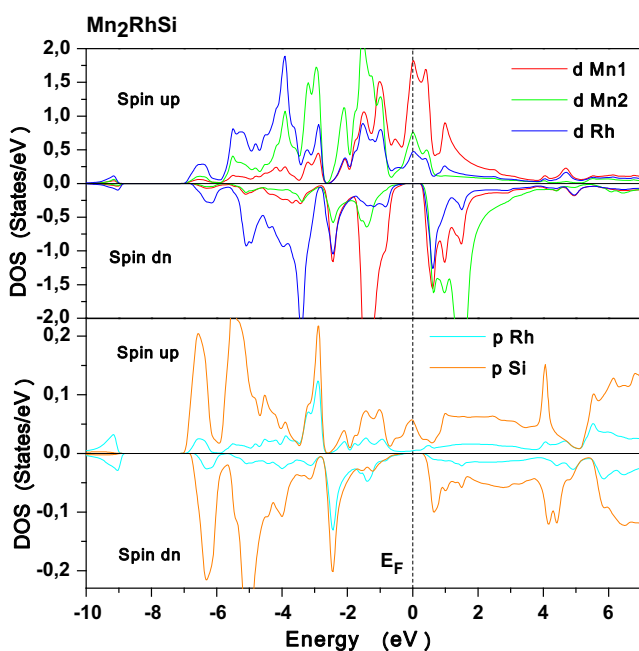


Fig. 5 Spin-polarized partial densities of states for Mn_2RhSi at equilibrium lattice constant

Furthermore, the majority-spin valence band is mainly dominated by the d -states of Mn_1 and Mn_2 atoms that hybridize with d (Rh) and p (Si) states as shown in Fig. 5. On the other hand, the conduction band is principally formed by the hybridization between d (Mn_1) and d (Mn_2) states. The d (Mn) states of majority spin shifted to higher energies and cross the Fermi level, while in the minority spin, a bandgap appears at E_F , between the occupied d (Mn) bonding states and the unoccupied d (Mn) antibonding states. This leads to a bandgap at E_F in the minority-spin states and a metallic character at E_F in the majority-spin states, which means that Mn_2RhSi is half-metal with spin polarization of 100 %. Therefore, the Mn_2RhSi material seems to be a potential candidate for spintronic applications.

It is well known that the lattice constant can undergo a considerable variation due to strain and thus deviates from its equilibrium value. This is widely influenced by the half-metallic property for spintronic applications. It is therefore useful to study the variation of the half-metallicity of Mn_2RhSi with respect to the lattice constant. However, the half-metallic behavior of our compound is now examined when the lattice constant is changed. For this purpose, the spin-polarized total density of states of Mn_2RhSi Heusler alloy is calculated for the different values of the lattice parameter in the range of 5.65 to 6.01 Å. Figure 6 illustrates the TDOS of Mn_2RhSi as a function of the lattice constant. The whole structure of the TDOS shifted to higher energies towards the Fermi level. The majority-spin states

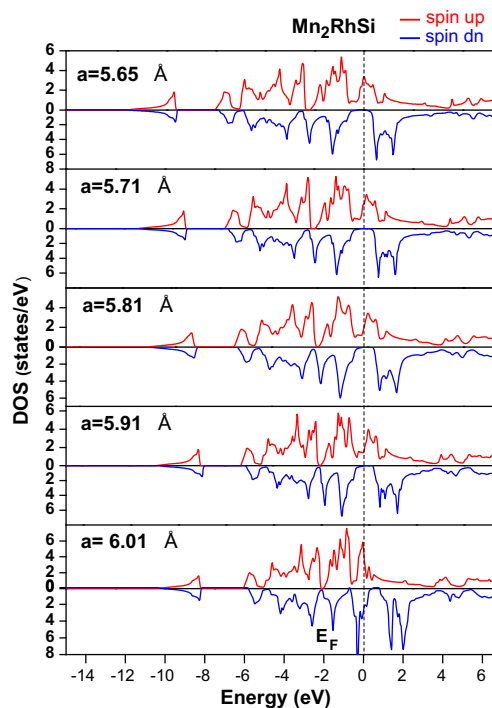


Fig. 6 Spin-polarized total densities of states for Mn_2RhSi in the range 5.65 to 6.01 Å of lattice constant

Table 4 Calculated total and partial magnetic moments for Mn₂RhSi

Compound	Total (μ_B)	Mn ₁ (μ_B)	Mn ₂ (μ_B)	Rh (μ_B)	Si (μ_B)	Interstitial (μ_B)
Mn ₂ RhSi	3.00	−0.409	3.013	0.296	0.016	0.085
Other calculations [33]						
Mn ₂ RhSi	3.00	−0.50	3.16	0.32	0.02	

exhibit only minor changes in shape as the lattice constant varies, but the position of the DOS of minority spin shifted towards a higher energy with increasing of the lattice constant (a) and cross the Fermi level when $a = 6.01 \text{ \AA}$. Thus, the Mn₂RhSi Heusler alloy is half-metal in the range 5.65 to 5.91 \AA of the lattice constant, but this compound reveals a metallic behavior at the lattice constant equal to 6.01 \AA .

3.3 Magnetic Properties

The calculated total and partial magnetic moments of Mn₂RhSi Heusler alloy are summarized in Table 4. The computed total magnetic moment is compared to the total magnetic moment with respect to the Slater-Pauling rule. The total magnetic moment (M_t) at the equilibrium lattice parameter for Mn₂RhSi is an integral number of $3 \mu_B$, which follows the Slater-Pauling rule of $M_t = Z_t - 24 = 3 \mu_B$, where Z_t is the number of valence electrons [13].

Our calculations show that Rh atoms have positive magnetic moments, whereas the Mn atoms have antiparallel spin moments. As is often the case, when these transition metals are very close to each other, there is an antiparallel coupling in space. Thus, there is a strong correlation between the lattice parameter and the interaction between magnetic spins of atoms. However, the magnetic alignment of Mn₁ and Mn₂ atoms is antiparallel with magnetic moments of $-0.409 \mu_B$ of Mn₁ and $3.013 \mu_B$ of Mn₂. As a consequence, the Mn₂RhSi exhibits a half-metallic ferrimagnetic behavior.

4 Conclusion

In summary, we have investigated the structural, elastic, electronic and magnetic properties of the Mn₂RhSi of Heusler alloy, using the firstprinciples calculations of the fullpotential linearized augmented plane wave (FP-LAPW) method. From structural and elastic properties, we found that this compound is stable in the Hg₂CuTi-type structure. The Mn₂RhSi exhibits a half-metallic ferrimagnetic character at equilibrium lattice constant, and this behavior results from the antiparallel magnetic alignment of Mn₁ and Mn₂ atoms. The total magnetic moment of Mn₂RhSi is an integral Bohr magneton of $3 \mu_B$, which obeys to the Slater-Pauling rule and confirms the half-metallicity of

this material. From our findings, we have predicted that Mn₂RhSi Heusler alloy is a potential candidate for practical spintronic applications.

References

- Julliere, M.: Phys. Lett. A **54**, 225 (1975)
- Jimbo, M., Kanda, T., Goto, S.: J. Magn. Magn. Mater. **126**, 422 (1993)
- Ohno, H.: Science **281**, 951 (1998)
- Heusler, F., Deut, V.: Phys. Ges. **5**, 219 (1903)
- Webster, P.J., Ziebeck, K.R.A.: Alloys and compounds of d-elements with main group elements. Part 2. In: Wijn, H.R.J. (ed.) Landolt-Börnstein, New Series, Group III, Pt.c, vol. 19, p. 75184. Springer, Berlin
- Pierre, J., Skolozdra, R.V., Tobola, J., Kaprzyk, S., Hordequin, C., Kouacou, M.A., Karla, I., Currat, R., Lelièvre-Berna, E.: J. Alloys Compd. **262**, 101 (1997)
- Tobola, J., Pierre, J.: J. Alloys Compd. **296**, 243 (2000)
- Hichour, M., Rached, D., Khenata, R., Rabah, M., Merabet, M., Reshak, A.H., Bin Omran, S., Ahmed, R.: J. Phys. Chem. Solids **73**, 975 (2012)
- Liu, G.D., Dai, X.F., Yu, S.Y., Zhu, Z.Y., Chen, J.L., Wu, G.H., Zhu, H., Xiao, J.Q.: Phys. Rev. B **74**, 054435 (2006)
- Weht, R., Pickett, W.E.: Phys. Rev. B **60**, 13006 (1999)
- Ishida, S., Asano, S., Ishida, J.: J. Phys. Soc. Jpn. **53**, 2718 (1984)
- Itoh, H., Nakamichi, T., Yamaguchi, Y., Kazama, N.: Trans. Jpn. Inst. Met. **24**, 265 (1983)
- Wurmehl, S., Kandpal, H.C., Fecher, G.H., Felser, C.: J. Phys. Condens. Matter **18**, 6171 (2006)
- Al-zyadi, J.M.K., Gao, G.Y., Yao, K.L.: J. Alloys Compd. **565**, 17 (2013)
- Liu, G.D., Dai, X.F., Liu, H.Y., Chen, J.L., Li, Y.X., Xiao, G., Wu, G.H.: Phys. Rev. B **77**, 014424 (2008)
- Luo, H., Zhu, Z., Ma, L., Xu, S., Zhu, X., Jiang, C., Xu, H., Wu, G.: J. Phys. D Appl. Phys. **41**, 055010 (2008)
- Dai, X.F., Liu, G.D., Chen, J.L., Wu, G.H.: Solid State Commun. **140**, 533 (2006)
- Luo, H.Z., Zhang, H.W., Zhu, Z.Y., Ma, L., Xu, S.F., Wu, G.H., Zhu, X.X., Jiang, C.B., Xu, H.B.: J. Appl. Phys. **103**, 083908 (2008)
- Barman, S.R., Chakrabarti, A.: Phys. Rev. B **77**, 176401 (2008)
- Luo, H., Liu, G., Feng, Z., Li, Y., Ma, L., Wu, G., Zhu, X., Jiang, C., Xu, H.: J. Magn. Magn. Mater. **321**, 4063 (2009)
- Fujii, S., Okada, M., Ishida, S., Asano, S.: J. Phys. Soc. Jpn. **77**, 74702 (2008)
- Luo, H.Z., Zhu, Z.Y., Liu, G.D., Xu, S.F., Wu, G.H., Liu, H.Y., Qu, J.P., Li, Y.X.: J. Magn. Magn. Mater. **320**, 421 (2008)
- Xing, N.S., Li, H., Dong, J.M., Long, R., Zhang, C.W.: Comp. Mater. Sci. **42**, 600 (2008)
- Luo, H., Liu, G., Feng, Z., Li, Y., Ma, L., Wu, G., Zhu, X., Jiang, C., Xu, H.: J. Magn. Magn. Mater. **321**, 4063 (2009)

25. Wei, X.P., Hu, X.R., Mao, G.Y., Chu, S.B., Lei, T., Hu, L.B., Deng, J.B.: *J. Magn. Magn. Mater.* **322**, 3204 (2010)
26. Luo, H.Z., Meng, F.B., Feng, Z.Q., Li, Y.X., Zhu, W., Wu, G.H., Zhu, X.X., Jiang, C.B., Xu, H.B.: *J. Appl. Phys.* **105**, 103903 (2009)
27. Wei, X.P., Deng, J.B., Chu, S.B., Mao, G.Y., Hu, L.B., Yang, M.K., Hu, X.R.: *Comp. Mater. Sci.* **50**, 1175 (2011)
28. Luo, H.Z., Liu, G.D., Meng, F.B., Wang, L.L., Liu, E.K., Wu, G.H., Zhu, X.X., Jiang, C.B.: *Comp. Mater. Sci.* **50**, 3119 (2011)
29. Wei, X.P., Hu, X.R., Liu, B., Lei, Y., Deng, H., Yang, M.K., Deng, J.B.: *J. Magn. Magn. Mater.* **323**, 1606 (2011)
30. Pickett, W.E., Moodera, J.S.: *Phys. Today* **54**, 39 (2001)
31. Zenasnia, H., Faraoun, H.I., Esling, C.: *J. Magn. Magn. Mater.* **333**, 162 (2013)
32. Bensaid, D., Hellal, T., Ameri, M., Azzaz, Y., Doumi, B., Al-Douri, Y., Abderrahim, B., Benzoudji, F.: *J. Supercond. Nov. Magn.* **29**, 1843 (2016)
33. Ren, Z., Liu, Y., Li, S., Zhang, X., Liu, H.: *Mater. Sci-Poland.* doi:[10.1515/msp-2016-0043](https://doi.org/10.1515/msp-2016-0043)
34. Blaha, P., Schwarz, K., Madsen, G.K.H., Kvasnicka, D., Luitz, J.: *WIEN2k, An Augmented Plane Wave Plus Local Orbitals Program for Calculating Crystal Properties.* Vienna University of Technology, Vienna (2001)
35. Perdew, J.P., Burke, K., Ernzerhof, M.: *Phys. Rev. Lett.* **77**, 3865 (1996)
36. Mehl, M.J., Osburn, J.E., Papaconstantopoulos, D.A., Klein, B.M.: *Phys. Rev. B* **41**, 10311 (1990)
37. Mehl, M.J.: *Phys. Rev. B* **47**, 2493 (1993)
38. Wang, J., Yip, S., Phillpot, S.R., Wolf, D.: *Phys. Rev. Lett.* **71**, 4182 (1993)
39. Nye, F.J.: *Physical Properties of Crystals.* Oxford University Press, Oxford (1985)
40. Karki, B.B., Ackland, G.J., Crain, J.: *J. Phys. Condens. Matter* **9**, 8579 (1997)